# Thermal poling of multi-wire array optical fiber

**Huang, Lin; An, Honglin; Hayashi, Juliano G.; Ren, Guobin; Stefani, Alessio ; Fleming, Simon**

*Published in:*
Optics Express

*Link to article, DOI:*
10.1364/OE.26.000674

*Publication date:*
2018

*Document Version*
Publisher's PDF, also known as Version of record

Research Article | Vol. 26, No. 2 | 22 Jan 2018 | OPTICS EXPRESS 674
Optics EXPRESS

# Thermal poling of multi-wire array optical fiber

LIN HUANG,[1,2] HONGLIN AN,[1] JULIANO G. HAYASHI,[1] GUOBIN REN,[2] ALESSIO STEFANI,[1,3] AND SIMON FLEMING[1,*]

[1]*Institute of Photonics and Optical Science (IPOS), School of Physics, The University of Sydney, NSW, 2006, Australia*
[2] *Key Lab of All Optical Network & Advanced Telecommunication Network of EMC, Beijing Jiaotong University, Beijing 100044, China*
[3]*DTU Fotonik, Department of Photonics Engineering, Technical University of Denmark, DK-2800 Kgs. Lyngby, Denmark*
**simon.fleming@sydney.edu.au*

**Abstract:** We demonstrate in this paper thermal poling of multi-wire array fibers, which extends poling of fibers with two anodes to ~50 and ~500 wire array anodes. The second harmonic microscopy observations show that second order nonlinearity (SON) layers are developed surrounding all the rings of wires in the ~50 anode array fiber with poling of 1.8kV, 250°C and 30min duration, and the outer rings of the ~500 anode array fiber at lower poling temperature. Our simulations based on a two-dimensional charge dynamics model confirm this can be explained by the self-adjustment mechanism, and show the SON layers are induced from the outer rings to the inner rings.



**OCIS codes:** (190.4160) Multiharmonic generation; (190.4370) Nonlinear optics, fibers; (190.4400) Nonlinear optics, materials; (160.3918) Metamaterials.

## References and links

1. R. A. Myers, N. Mukherjee, and S. R. J. Brueck, "Large second-order nonlinearity in poled fused silica," Opt. Lett. **16**(22), 1732–1734 (1991).
2. T. G. Alley, S. R. J. Brueck, and R. A. Myers, "Space charge dynamics in thermally poled fused silica," J. Non-Cryst. Solids **242**(2), 165–176 (1998).
3. A. Le Calvez, E. Freysz, and A. Ducasse, "Experimental study of the origin of the second-order nonlinearities induced in thermally poled fused silica," Opt. Lett. **22**(20), 1547–1549 (1997).
4. X. C. Long, R. A. Myers, and S. R. J. Brueck, "A poled electrooptic fiber," IEEE Photonics Technol. Lett. **8**(2), 227–229 (1996).
5. P. G. Kazansky, L. Dong, and P. S. J. Russell, "High second-order nonlinearities in poled silicate fibers," Opt. Lett. **19**(10), 701–703 (1994).
6. W. Xu, P. Blazkiewicz, and S. Fleming, "Silica Fiber Poling Technology," Adv. Mater. **13**(12–13), 1014–1018 (2001).
7. P. G. Kazansky and P. S. J. Russel, "Thermally poled glass: frozen-in electric field or oriented dipoles?" Opt. Commun. **110**(5), 611–614 (1994).
8. W. Margulis, O. Tarasenko, and N. Myrén, "Who needs a cathode? Creating a second-order nonlinearity by charging glass fiber with two anodes," Opt. Express **17**(18), 15534–15540 (2009).
9. H. An and S. Fleming, "Investigating the effectiveness of thermally poling optical fibers with various internal electrode configurations," Opt. Express **20**(7), 7436–7444 (2012).
10. A. Tuniz, B. T. Kuhlmey, R. Lwin, A. Wang, J. Anthony, R. Leonhardt, and S. C. Fleming, "Drawn metamaterials with plasmonic response at terahertz frequencies," Appl. Phys. Lett. **96**(19), 191101 (2010).
11. A. Tuniz, R. Lwin, A. Argyros, S. C. Fleming, and B. T. Kuhlmey, "Fabricating metamaterials using the fiber drawing method," J. Vis. Exp. **68**, e4299 (2012).
12. S. Atakaramians, A. Stefani, H. Li, M. S. Habib, J. G. Hayashi, A. Tuniz, X. Tang, J. Anthony, R. Lwin, A. Argyros, S. C. Fleming, and B. T. Kuhlmey, "Fiber-Drawn Metamaterial for THz Waveguiding and Imaging," J. Infrared. Millim. Te. **39**(8), 1162–1178 (2017).
13. E. J. Smith, Z. Liu, Y. Mei, and O. G. Schmidt, "Combined Surface Plasmon and Classical Waveguiding through Metamaterial Fiber Design," Nano Lett. **10**(1), 1–5 (2010).
14. S. Fleming, A. Stefani, X. Tang, A. Argyros, D. Kemsley, J. Cordi, and R. Lwin, "Tunable metamaterials fabricated by fiber drawing," J. Opt. Soc. Am. B **34**(7), D81–D85 (2017).
15. A. Camara, O. Tarasenko, and W. Margulis, "Study of thermally poled fibers with a two-dimensional model," Opt. Express **22**(15), 17700–17715 (2014).

#314510 https://doi.org/10.1364/OE.26.000674
Journal © 2017 Received 29 Nov 2017; revised 29 Dec 2017; accepted 31 Dec 2017; published 8 Jan 2018

Optics EXPRESS

16. L. Huang, G. Ren, and X. Sun, "Evolution of Two-dimensional Electric Field in Poled Twin-hole Optical Fiber," in *International Photonics and OptoElectronics Meetings*, OSA Technical Digest (online) (Optical Society of America, 2014), FTh2F.5.
17. J. Hayashi, *Wire Array Infrared Metamaterial Fibres: Fabrication and Applications*, PhD, University of Sydney (2017) (A journal paper is in preparation)
18. P. Russell, "Photonic Crystal Fibers," Science **299**(5605), 358–362 (2003).
19. S. Tomotika, "On the instability of a cylindrical thread of a viscous liquid surrounded by another viscous fluid," Proc. R. Soc. Lond. A Math. Phys. Sci. **150**(870), 322–337 (1935).
20. H. An, S. Fleming, and G. Cox, "Visualization of second-order nonlinear layer in thermally poled fused silica glass," Appl. Phys. Lett. **85**(24), 5819–5821 (2004).
21. H. An and S. Fleming, "Near-anode phase separation in thermally poled soda lime glass," Appl. Phys. Lett. **88**(18), 181106 (2006).
22. F. De Lucia, D. Huang, C. Corbari, N. Healy, and P. J. A. Sazio, "Optical fiber poling by induction," Opt. Lett. **39**(22), 6513–6516 (2014).
23. F. De Lucia, D. Huang, C. Corbari, N. Healy, and P. J. A. Sazio, "Optical fiber poling by induction: analysis by 2D numerical modeling," Opt. Lett. **41**(8), 1700–1703 (2016).

## 1. Introduction

Thermal poling can break macroscopic centrosymmetry of silica glasses and create second-order nonlinearity (SON), $\chi^{(2)}$, in glasses [1–3] and waveguides [4–6]. When applied with high voltage across the sample at elevated temperature, mobile alkali metal ions in the glass matrix are activated by the high temperature and swept by the field away from the anode, resulting in a depletion region near the anode. This is subsequently followed by migration of a second kind of charge driven by the strong internal electric field in the depletion region, which results in the movement of the depletion region. When poling is complete, i.e., the sample is cooled down to room temperature and then the applied voltage is switched off, the unbalanced distribution of charges induces a strong frozen-in electric field, $E_{rec}$. The $\chi^{(2)}$ is obtained through coupling $E_{rec}$ to the intrinsic third order optical nonlinearity, $\chi^{(3)}$, $\chi^{(2)} = 3E_{rec}\chi^{(3)}$ [2, 7].

The mobile charges are driven by the electric field. However, in the two-anode poled twin-holes fibers, when the two electrodes are at the same positive voltage, a counterintuitive observation was obtained that a much stronger and temperature stable SON layer was created between the two anodes [8, 9]. While the electric field should be small between the two anodes when the same potential is applied, an avalanche-like positive feedback mechanism happens during the two-anode poling process [8]. As fibers can accommodate more holes and thus, more electrodes, it is interesting to explore how far this thermal poling can be extended from just two anodes, and the extent to which an induced SON can be distributed through the volume of the glass. Such fibers are available due to recent advances in using fiber drawing for fabricating metamaterials with arrays of tens to hundreds of metal wires [10–13]. Poling these structures and inducing a SON may enable tunable metamaterials [14] with potential applications in sub-diffraction imaging and waveguide devices. In this paper, we demonstrate experimentally thermal poling of fibers of~50 and ~500 tin wire array anodes, arranged in concentric rings. SON layers are created surrounding the wire rings. Simulation of the thermal poling process based on a two-dimensional charge dynamics model [15, 16] are conducted to illuminate the physical mechanism involved.

## 2. Fabrication and thermal poling of multi-wire array optical fiber

The multi-wire array fibers shown in this work were fabricated by a development [17] of a technique used for the drawing of metamaterial preforms [11]. This involved macroscopic versions of the wire array structures, which were obtained by the conventional stack-and-draw technique [18] and a pressure-assisted metal filling process. The drawing parameters employed were optimized to avoid fluid dynamic instabilities in the scaling down process, which can generate fluctuations in the metallic structure and breakage of the wires [19], particularly for wires with diameters below a couple of microns. The glass is AR-GLAS from Schott and its chemical composition in weight % is: $SiO_2$(69%), $B_2O_3$(1%), $K_2O$(3%),

Optics EXPRESS

$Al_2O_3$(4%), $Na_2O$(13%), BaO(2%), CaO(5%), MgO(3%). The diameter of the fiber and the tin filled holes are ~1000μm, and ~10μm, respectively, and the pitch of the tin filled holes is ~20μm.

The internal tin wires in the fiber were connected to tungsten wire using conductive silver adhesive. The fiber end faces were carefully cleaved to optimize the connection, and then put in the conductive silver adhesive attempting to ensure good coverage of the adhesive to the fiber end face, however it was not possible to be certain that all wires were contacted by the adhesive. A tungsten wire was then inserted into the silver adhesive close to the fiber end face. A strong connection between the tungsten wire and the tin wires was obtained when the adhesive was dry. During poling the fibers were placed on an electrically grounded hotplate at high temperature. To avoid thermal runaway and dielectric breakdown, the poling voltage was increased from 500V to 1.8kV with a step of 100V every 2min. 1.8kV DC voltage was applied to the tungsten wire for 30min. The ~50 and ~500 wire fibers were poled at 210°C, and a second ~50 wire fiber was poled at 250°C for comparison. It should be noted that voltage breakdown occurred in the ~500 wire fiber when poled at higher temperature (250°C) or higher voltage (2kV). After poling, the samples were cooled down to room temperature before the voltage was switched off.

The poled samples were characterized using second harmonic (SH) microscopy. A detailed description of this experimental technique is reported in [20]. The microscope is equipped with dual photomultiplier detectors to capture both the ordinary optical images in channel one and SH images in channel two. The microscope is also equipped with a 505 DCLP dichroic mirror to divide the detectable spectrum (380–680 nm) at 505 nm between the two channels. To obtain information about the spatial distribution of the induced SON, overlay images were obtained by simultaneously capturing micrographs in both channels from the same sample area of interest. The resolution was estimated to be ~0.4μm.

## 3. Experimental results

Typical SH microscope images of the poled ~50 wire fiber poled at 1.8kV, 210°C for a duration of 30min are shown in Fig. 1. Figure 1(a) (“channel two”) shows that SH signals were found in rings around most of the holes. Whilst these measurements were not directly calibrated, comparison to other calibrated measurements shows the magnitude is lower than, but comparable to, those observed in poled soda-lime glass [21] and silica fibers [8,9] (less than 0.1pm/V). Several holes are not well poled, presumably due to some poor connections between the tungsten wire and the tin wires and potentially discontinuity of the tin wire formed in the drawing process. The same fiber was poled at higher temperature, as shown in Fig. 2(a). Compared with the results in Fig. 1(a), SH signals were clearly enhanced (almost doubled based on analysis of the measured values). The intensities of the SH signals in Fig. 2(a) are comparable to those observed in poled silica fiber. Note that since *y*-polarized light is used in the SH microscopy, the observed SH signals are strong along the *y*-direction while weak along the *x*-direction. The poled ~500 wire fiber in Fig. 3 shows the SH signals are induced in the glass proximal to the wires making up the outer rings of wires with the largest intensity stronger than the results in Fig. 1(a) but lower than that in Fig. 2(a)

The overlay images in Fig. 1(b) and Fig. 2(b) show that the SH signals are generated just underneath the surface of the holes, and after a poling period of 30 min they have a width of ~1μm. This observation, combined with the strong dependency of SH intensity on poling temperature, is consistent with the accepted mechanism of poling (rather than perhaps being due to polarization in the metal glass interface). More specifically we can conclude that the alkali metal ions are the dominant charges migrating during poling. The enhancement of the SH signal intensity at higher temperature is also consistent with short poling duration results [2], during which the depletion region is formed gradually, and the migration of the following second kind of mobile charges can be neglected.

Optics EXPRESS

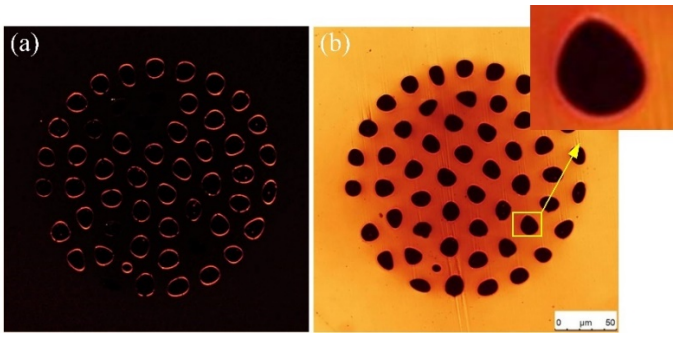


Fig. 1. SH micrographs of the fiber poled at 210°C, 1.8kV for 30min. (a) SH signals and (b) overlay of images of the cross-section of the multi-hole array and SH signals. The inset in (b) shows the zoomed in SH signals around one wire.

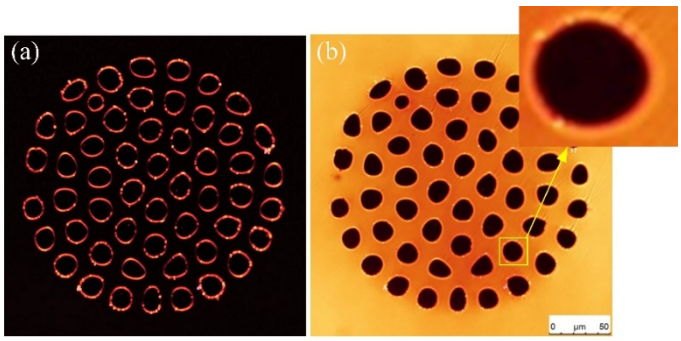


Fig. 2. SH micrographs of the fiber poled at 250°C, 1.8kV for 30min. (a) SH signals and (b) overlay of images of the cross-section of the multi-hole array and SH signals. The inset in (b) shows the zoomed in SH signals around one wire. Note that the tin (melting temperature ~232°C,) is liquid at poling temperature 250°C, potentially improving the continuity of the tin wires in the fiber.

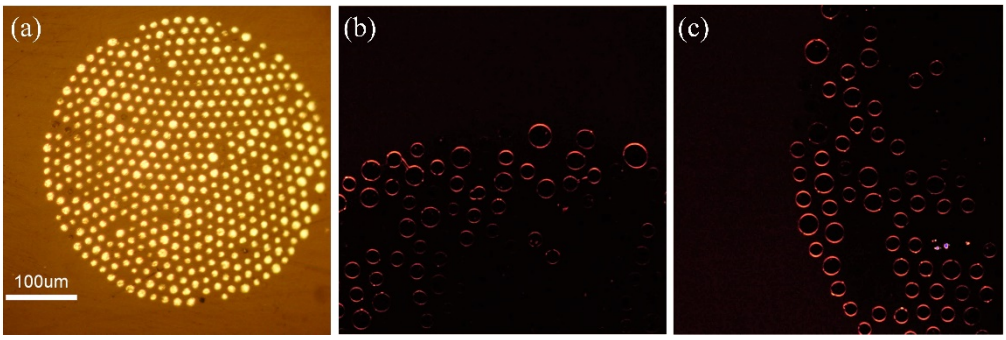


Fig. 3. (a) Cross-section of the ~500 wire fiber. After poling at 210°C, 1.8kV and 30min duration, only the outer wire rings are poled: the SH signal from (b) the upper part and (c) the left part of the poled ~500 wire fiber.

The results shown in Fig. 1 and Fig. 2 are apparently quite anomalous, because if all the wires are at the same potential it might be expected that the outer ring of wires would effectively screen the inner wires and there would be no field within this ring, and just radial fields from the outer ring. This observed pattern however can be explained by referring to the avalanche-like positive feedback mechanism [8] or the similar “self-adjustment” mechanism [9]. The migration of charges starts from the outer wire rings, where the strength of the electric field is initially relatively strong, this process creates local depletion regions in which

Optics EXPRESS

the resistivity is very high. This in turn causes a modification of the electric field distribution around the inner rings, and promotes the migration of charges in the inner rings.

## 4. Simulation results

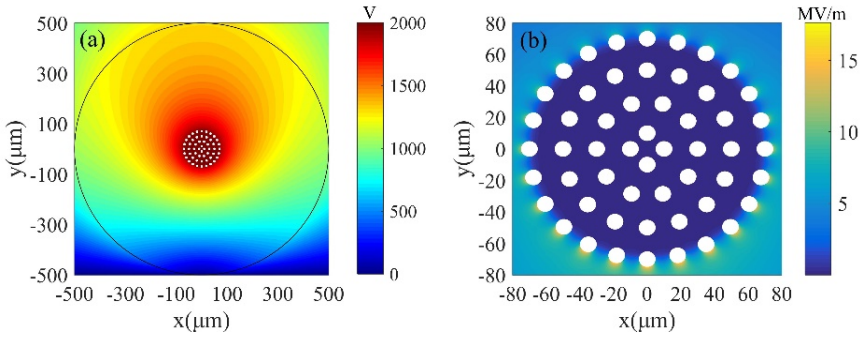


Fig. 4. Initial distribution of the (a) electric potential and (b) electric field in the ~50 wire fiber. The electrodes are applied with 2000V electric potential. See Visualization 1 and Visualization 2 for time evolution of electric potential and electric field in the ~50 wire fiber during poling.

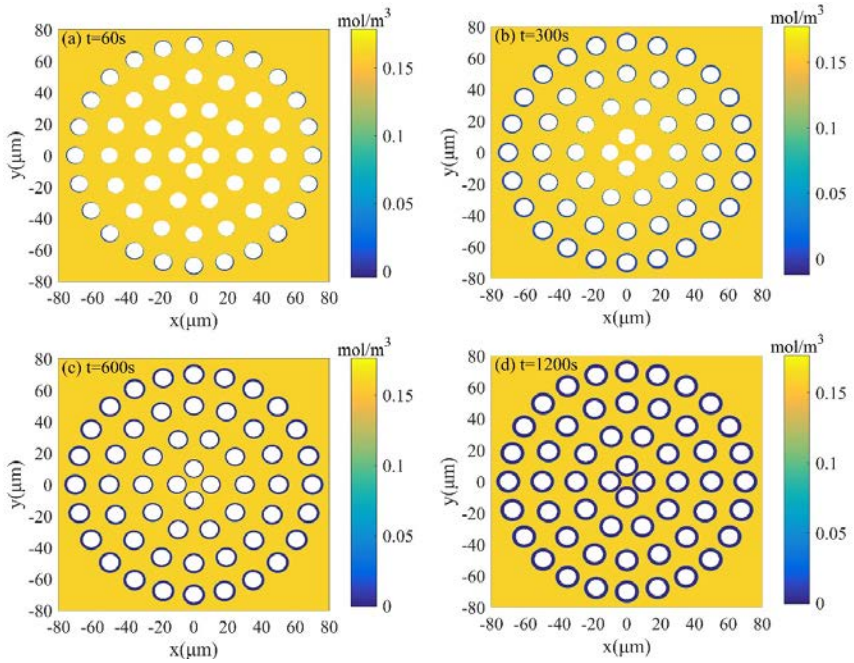


Fig. 5. Profile of $Na^+$ ions in the ~50 wire fiber at poling time (a) t = 60s, (b) t = 300s, (c) t = 600s, (d) t = 1200s. The poling temperature and voltage are 250°C and1.8kV, respectively. See Visualization 3 for time evolution of $Na^+$ in the ~50 wire fiber during poling.

We simulated the thermal poling process in the ~50 wire fiber based on a two-dimensional charge dynamics model using the finite element method. We assumed, based on the above discussion, that only alkali ions are involved, and modeled this by the migration of $Na^+$ ions with concentration of 0.16mol/$m^3$. The wires were assumed to be at 2kV potential, and a grounded plate and an 'air box' (2cm × 1cm) were adopted. The grounded plate was used to simulate the hot-plate in the experiment and the air box was used to simulate the surrounding air, and both are grounded at the edges [22, 23]. The electric potential in the ~50 wire fiber at t = 0s is shown in Fig. 4. Figure 4(a) shows the whole structure, and an electric potential

Optics EXPRESS

gradient is observed around the outer wire ring and is more obvious at the lower part since the lower surface is grounded. This strong potential gradient corresponds to the strong electric field around the outer wire ring, as shown in Fig. 4(b), while around the inner wire rings the strength of electric field is almost zero, as expected due to screening.

The migration process of $Na^+$ ions is shown in the simulated time sequence in Fig. 5, where the depletion region can be seen to develop around the outer wire rings first and then the inner rings. Finally, all wire rings have developed a depletion region, which is in accordance with our experimentally observed SH signal distributions in Fig. 1 and Fig. 2. With the electric field distribution at the initial poling time shown in Fig. 4 (b), a non-circular depletion region will be first developed around the outer rings as shown in Fig. 5, t = 60s. In the depletion region, resistivity grows rapidly and potential drops greatly, this modifies the electric field distribution from uniform to non-uniform, strong electric fields around the inner rings of wires appear gradually and drive the migration of charges. With poling continuing, a strong electric field appears at more regions and more depletion regions are developed, as illustrated in Fig. 5.

Although in these experiments the SON layers were only developed surrounding the outer rings of wire in the ~500 wire poling fiber, presumably all wires rings would develop SON layers with sufficiently long poling duration. It is also worth noting that the dielectric strength of soda-lime glass is lower than fused silica glass, hence we expect stronger SON may be achieved in poled multi-wire fused silica fibers than in soda-lime fiber.

## 5. Summary

In conclusion, we demonstrate experimentally poling ~50 and ~500 tin wire array fiber. The results show the ~50 wire fibers are successfully poled such that all rings of wires develop SON layers, and the SON enhances with increased poling temperature. SON layers were also observed surrounding the outer rings of wires in the ~500 wire fiber poled at lower poling temperature. Our simulation based on a two-dimensional charge dynamics model reveals the charge migration process in the multi-wire fiber. Although there is initially no electric potential drop in the inner wire rings, which would prevent charge migration in this region, the SON layers develop at the outer rings of wire at first, then the inner rings, and finally all wires are surrounded by an induced SON layer after sufficiently long poling time. This is in accordance with the self-adjustment mechanism in a two-anode poled fiber.

The findings extend poling of fiber from two anodes to multi anodes. Poled multi-wire fiber can be potentially applied for electro-optic modulation or frequency conversion, even a QPM structure may be obtained by using the multi-wire glass material from the side if the wires are removed. In addition, these results may also open up possibilities for tunable metamaterials.

## Funding

National Natural Science Foundation of China (NSFC) (61178008); Fundamental Research Funds for the Central Universities (2016YJS021); ARC Discovery Projects (DP130102348 & DP140104116); Marie Sklodowska-Curie grant of the European Union's Horizon 2020 research and innovation programme (708860).

## Acknowledgment

L. Huang acknowledges the support from China Scholarship Council (CSC). Juliano G. Hayashi would like to thank the Science without Borders Program by CAPES (Brazil) for the financial support under grant 9468/13-7. The authors acknowledge Boris T. Kuhlmey for helpful discussions.